1521-0111/83/4/770–780$25.00
MOLECULAR PHARMACOLOGY

http://dx.doi.org/10.1124/mol.112.081695
Mol Pharmacol 83:770–780, April 2013

Somatic Mutations in GRM1 in Cancer Alter Metabotropic Glutamate Receptor 1 Intracellular Localization and Signaling

Jessica L. Esseltine, Melinda D. Willard, Isabella H. Wulur, Mary E. Lajiness, Thomas D. Barber, and Stephen S. G. Ferguson

Molecular Brain Research Group, Robarts Research Institute and Department of Physiology and Pharmacology, University of Western Ontario, London, Ontario, Canada (J.L.E., S.S.G.F.); and Tailored Therapeutics, Eli Lilly and Company, Indianapolis, Indiana (M.D.W., I.H.W., M.E.H., T.D.B.)

Received August 2, 2012; accepted January 9, 2013

ABSTRACT

The activity of metabotropic glutamate receptors (mGluRs) is known to be altered as the consequence of neurodegenerative diseases such as Alzheimer, Parkinson, and Huntington disease. However, little attention has been paid to this receptor family's potential link with cancer. Recent reports indicate altered mGluR signaling in various tumor types, and several somatic mutations in mGluR1a in lung cancer were recently described. Group 1 mGluRs (mGluR1a and mGluR5) are coupled primarily to Gαq, leading to the activation of phospholipase C and to the formation of diacylglycerol and inositol 1,4,5-trisphosphate, leading to the release of Ca^{2+} from intracellular stores and protein kinase C (PKC) activation. In the present study, we investigated the intracellular localization and G protein–dependent and –independent signaling of eight *GRM1* (mGluR1a) somatic mutations. Two mutants found in close proximity to the glutamate binding domain and cysteine-rich region (R375G and G396V) show both decreased cell surface expression and basal inositol phosphate (IP) formation. However, R375G shows increased ERK1/2 activation in response to quisqualate stimulation. A mutant located directly in the glutamate binding site (A168V) shows increased quisqualate-induced IP formation and, similar to R375G, increased ERK1/2 activation. Additionally, a mutation in the G protein-coupled receptor kinase 2/PKC regulatory region (R696W) shows decreased ERK1/2 activation, whereas a mutation within the Homer binding region in the carboxyl-terminal tail (P1148L) does not alter the intracellular localization of the receptor, but it induces changes in cellular morphology and exhibits reduced ERK1/2 activation. Taken together, these results suggest that mGluR1a signaling in cancer is disrupted by somatic mutations with multiple downstream consequences.

Introduction

Metabotropic glutamate receptors (mGluRs) mediate the actions of the excitatory neurotransmitter glutamate. These class C receptors are characterized by a large extracellular amino-terminal glutamate binding region composed of two globular domains that form a distinctive "venus fly trap" (VFT) (Conn and Pin, 1997). The specific amino-terminal glutamate binding region has been identified as a stretch of 24 amino acids whose mutations affect glutamate affinity (O'Hara et al., 1993; Dhami and Ferguson, 2006). Adjacent to the VFT domain is a 70-amino-acid, cysteine-rich domain required for allosteric coupling between the VFT and the transmembrane domains (Huang et al., 2011). This region also participates in receptor dimerization via the formation of a cysteine bridge between receptor pairs, the disruption of which leads to receptor loss of function (Romano et al., 1996).

The second intracellular loop of mGluR is involved in G protein coupling and selectivity (Dingledine et al., 1999; Pin et al., 2003; Ferguson, 2007; Niswender and Conn, 2010). Group I mGluRs (mGluR1a and mGluR5) couple primarily through Gαq and also activate G protein–independent signal transduction pathways, including mitogen-activated kinases. Group I mGluR-mediated ERK1/2 activation can occur via protein kinase C (PKC), β-arrestin, nonreceptor tyrosine kinases, such as Src and Pyk2, and Homer (Thandi et al., 2002; Mao et al., 2005; Emery et al., 2010; Nicodemo et al., 2010).

Receptor activation is quickly followed by signal desensitization, a tightly regulated process essential to prevent aberrant signaling or chronic receptor overstimulation (Krupnick and Benovic, 1998; Ferguson, 2007). Desensitization of mGluRs is complex as mGluR1a desensitization includes phosphorylation-dependent and -independent mechanisms (Dhami et al., 2004, 2005; Dhami and Ferguson, 2006; Ferguson, 2007; Ribeiro et al., 2009). G protein-coupled receptor kinase 2

This work was supported by an operating grant from the Canadian Institutes of Health Research (CIHR) [MOP-111093]. S.S.G.F. also holds a Tier I Canada Research Chair in Molecular Neurobiology and is a Career Investigator of the Heart and Stroke Foundation of Ontario. J.L.E. is the recipient of an Ontario Graduate Scholarship.

J.L.E. and M.D.W. contributed equally to this work.

dx.doi.org/10.1124/mol.112.081695.

ABBREVIATIONS: DMEM, Dulbecco's modified Eagle's medium; GFP/YFP, green/yellow fluorescent protein; GPCR, G protein-coupled receptor; GRK, G protein-coupled receptor kinase; HA, hemagglutinin; HBSS, Hanks' balanced salt solution; HEK, human embryonic kidney; HRP, horseradish peroxidase; IP, inositol phosphate; mGluR1a, metabotropic glutamate receptor 1a; SNV, single nucleotide variant; VFT, venus fly trap.

(GRK2)-mediated mGluR1/5 desensitization is phosphorylation independent, whereas second-messenger–dependent kinases phosphorylate the second intracellular loop and carboxyl-terminal tail domains of mGluR1a to mediate phosphorylation-dependent mGluR desensitization (Francesconi and Duvoisin, 2000).

G protein-coupled receptor (GPCR) C-tails are responsible for association with many regulatory proteins involved in protein scaffolding or transport. For example, the Homer family of proteins is composed of three family members, each encoding multiple splice variants (Shiraishi-Yamaguchi and Furuichi, 2007). Homers associate with the PPxxFR motif in the C-tails of mGluR1a/5 via their amino-terminal ENA/VASP homology domains and regulate the subcellular distribution, plasma membrane target, and signaling of mGluR1a/5 (Roche et al., 1999; Tadokoro et al., 1999; Tu et al., 1999; Ango et al., 2002). Homer proteins tether mGluR1a/5 to the activation of IP receptors, ERK1/2 phosphorylation, and the modulation of ion channel activity (Kammermeier et al., 2000; Mao et al., 2005).

mGluRs were recently found to play a role in cancer progression (Teh and Chen, 2012). This finding is unsurprising as mGluRs can activate both MAPK and AKT, two of the hallmark signaling pathways that promote cancer growth, survival, invasion, and angiogenesis in tumors. Along these lines, overexpression and activating mutations of mGluR1, mGluR5, and mGluR3 in various cancer types—such as breast, melanoma, and renal cell carcinoma—have been shown to promote tumor development, growth, and progression, and pharmacologic inhibitors of these receptors correlate with reduced tumorigenesis (Pollock et al., 2003; Ohtani et al., 2008; Abdel-Daim et al., 2010; Choi et al., 2011; Prickett et al., 2011; Martino et al., 2012; Speyer et al., 2012). Thus, mGluRs appear to play a critical role in maintenance of the transformed phenotype and could be potential therapeutic targets for the treatment of several cancers.

Recently, whole-exome sequencing of multiple tumor types has identified more than 20 somatic missense mutations in the ligand binding and intracellular regulatory domains of mGluR1a (Table 1) (Sjoblom et al., 2006; Parsons et al., 2008; Kan et al., 2010). In the present study, we examined the effect of eight *GRM1* single-nucleotide variants (SNVs) identified in glioblastoma, lung, and colorectal cancer, including SNVs in the orthosteric glutamate binding region (D44E and A168V) and cysteine-rich region of the amino-terminal domain (R375G and G396V), intracellular loop 2 (R684C, R696W, and G688V), and Homer binding motif (P1148L) on mGluR1a signaling. Therefore, we asked the question of whether these naturally occurring mutations alter the expected signal transduction properties, protein interactions, and subcellular localization of mGluR1a. We found that a subset of these mutations results in altered mGluR1a-stimulated G protein

TABLE 1
Somatic mutations found in *GRM1* (mGluR1a) in cancers

Protein Change	Type	Location	Cancer Subtype	Reference
S33L	Missense	LB	Upper aerodigestive tract, squamous cell	Durinck et al., 2011
*D44E	Missense	LB	Lung, adeno	Kan et al., 2010
R71K	Missense	LB	Skin, squamous	Durinck et al., 2011
R78H	Missense	LB	Ovary, serous	CGARN, 2011
D87H	Missense	LB	Ovary, serous	CGARN, 2011
A91T	Missense	LB	Large intestine, adeno	TCGA
K153N	Missense	LB	Large intestine, adeno	TCGA
*A168V	Missense	LB	Lung, adeno	Kan et al., 2010
A184T	Missense	LB	Hematopoietic and lymphoid tissue, chronic lymphocytic leukemia-small lymphocytic lymphoma	Quesada et al., 2011
W224C	Missense	LB	Ovary, serous	CGARN, 2011
A229S	Missense	LB	Ovary, serous	CGARN, 2011
R275H	Missense	LB	Large intestine, adeno	TCGA
R297	Nonsense	LB	Breast, ductal	
*R375G	Missense	LB	Lung, squamous cell	Kan et al., 2010
E386	Nonsense	LB	Lung, adeno	Kan et al., 2010
*G396V	Missense	LB	Lung, adeno	Kan et al., 2010
I414V	Missense	LB	Large intestine, adeno	TCGA
P444L	Missense	LB	Upper aerodigestive tract, squamous cell	Stransky et al., 2011
C547F	Missense	LB	Skin, squamous	Durinck et al., 2011
D619A	Missense	il1	Breast, basal, triple-negative	Shah et al., 2012
S626C	Missense	il1	CNS, astrocytoma grade IV	CGARN, 2008
T655N	Missense	ex2	Large intestine, adeno	TCGA
R661H	Missense	ex2	Large intestine, adeno	TCGA
*R684C	Missense	il2	CNS, astrocytoma grade IV	Parsons et al., 2008
*G688V	Missense	il2	Lung, squamous cell	Kan et al., 2010
*R696W	Missense	il2	Large intestine, adeno	Sjöblom et al., 2006; Wood et al., 2007
Q706	Nonsense	il2	Upper aerodigestive tract	Durinck et al., 2011
N782I	Missense	il3	Large intestine, adenocarcinoma	TCGA
S783I	Missense	il3	Breast, basal, triple-negative	Shah et al., 2012
R967H	Missense	C-tail	CNS, astrocytoma grade IV	CGARN, 2008
E1006K	Missense	C-tail	Skin, squamous	Durinck et al., 2011
D1096N	Missense	C-tail	Ovary, serous carcinoma	CGARN, 2011
P1148L	Missense	C-tail	Large intestine, adeno	Wood et al., 2007

Adeno, adenocarcinoma; CNS, central nervous system.
* Mutations characterized in the manuscript.

coupling, biased ERK1/2 phosphorylation, intracellular retention in the endoplasmic reticulum (ER), and a loss of Homer binding. Each of these alterations in mGluR1a signaling phenotype has the potential to contribute to altered receptor activity in cancer.

Materials and Methods

Materials. We acquired *myo*-(^{3}H)inositol from PerkinElmer Life Sciences (Waltham, MA). Dowex 1-X8 (formate form) resin 200–400 mesh was purchased from BioRad (Mississauga, ON, Canada). Normal donkey serum was purchased by Jackson ImmunoResearch (West Grove, PA). ECL Western blotting detection reagents were purchased from GE Healthcare (Oakville, ON, Canada). Horseradish peroxidase-conjugated anti-rabbit and anti-goat IgG secondary antibody were obtained from BioRad, and anti-mGluR1a rabbit polyclonal antibody was purchased from Upstate (Lake Placid, NY). Rabbit polyclonal phospho-p42/44 MAP kinase (Thr202/Tyr402), p42/44 MAP kinase antibodies were obtained from Cell Signaling Technology (Pickering, ON, Canada). Alexa Fluor 488 donkey anti-Rabbit IgG, Alexa Fluor 568 donkey anti-rabbit IgG and Zenon Rabbit Alexa Fluor 555 were purchased from Invitrogen/Molecular Probes (Burlington, ON, Canada). Rabbit anti-FLAG antibody, M2 anti-FLAG agarose, Rabbit anti-hemagglutinin (HA) antibody and all other biochemical reagents were purchased from Sigma-Aldrich (Oakville, ON, Canada).

DNA Construction. To create the pcDNA3.1(+)/FLAG-mGluR1a constructs, amino acids 19–1194 of human mGluR1a were cloned in-frame with the signal peptide from the transmembrane receptor CD33 (amino acids 1–15), followed by a single FLAG tag (DYKDDDDK). Site-directed mutagenesis was performed using the QuikChange system (Stratagene, Wilmington, DE) to generate the following mutants of mGluR1a: D44E, A168V, R375G, G396V, R684C, G688V, R696W, and P1148L.

Cell Culture. Human embryonic kidney (HEK) 293 cells were maintained in Eagle's minimal essential medium supplemented with 8% (v/v) heat inactivated fetal bovine serum and 50 μg/ml of gentamicin. Cells seeded in 100-mm dishes were transfected using a modified calcium phosphate method as described previously (Dale et al., 2001). After transfection (18 hours), the cells were incubated with fresh medium and allowed to recover for 24 hours for coimmunoprecipitation studies. Otherwise, they were allowed to recover for 6–8 hours and reseeded into 12-well or 24-well dishes and then grown an additional 18 hours before experimentation.

ERK1/2 Activation and Western Blotting. HEK 293 cells were transiently transfected with the cDNAs described in the figure legends; 48-hour post-transfection cells were serum starved overnight in glutamine-free Dulbecco's modified Eagle's medium (DMEM) and stimulated for the indicated times with 30 μM quisqualate. The cells were then placed on ice, washed twice with ice-cold phosphate-buffered saline, and lysed with cold-lysis buffer (50 mM Tris, pH 8.0, 150 mM NaCl, 0.1% Triton X-100) containing protease inhibitors (1 mM 4-(2-aminoethyl)benzenesoltonyl fluoride hydrochloride, 10 μg/ml of leupeptin, and 5 μg/ml of aprotinin) and phosphatase inhibitors (10 mM NaF, 5 μM Na_3VO_4). The cells were placed on a rocking platform for 15 minutes at 4°C and centrifuged at 15,000*g* for 15 minutes at 4°C to pellet insoluble material. Cell extracts were solubilized in a 3× SDS sample buffer containing 2-mercaptoethanol (BME). Samples were separated by SDS-PAGE, transferred to a nitrocellulose membrane, and immunoblotted to identify phosphorylated (active) and total p42/44 (ERK1/2) (1:1000 dilution; Cell Signaling) followed by a horseradish peroxidase-conjugated secondary anti-rabbit (1:10,000; BioRad). Receptor protein expression was determined by immunoblotting 10 μg of protein from each cell lysate. Proteins were detected using chemiluminescence with the ECL kit from GE Healthcare.

Coimmunoprecipitation. Transfected HEK 293 cells were lysed for 48 hours post-transfection in cold radioimmunoprecipitation buffer (150 mM NaCl, 1% IGEPAL CA-630, 0.5% sodium deoxycholate, 0.1% SDS, 50 mM Tris pH 8.0; Sigma-Aldrich) plus protease inhibitors (complete EDTA-free; Roche, Mississauga, ON, Canada). Cell lysates were sonicated in an ice-water bath for 5 minutes and then centrifuged at 16,500*g* for 20 minutes at 4°C. A portion of the supernatant was removed and mixed 1:1 with 6× Laemmli sample buffer ("lysate" samples). Anti-FLAG was used to immunoprecipitate mGluR1a from resultant lysates; 48 hours post-transfection, co-immunoprecipitating proteins and total lysates resolved by SDS-PAGE were immunoblotted with anti-M2-FLAG-horseradish peroxidase (HRP), anti-3F10-HA-HRP, or anti-yellow fluorescent protein antibodies. Samples were subjected to SDS-PAGE and transferred to nitrocellulose using the iBlot dry blotting system. Membranes were blocked in 5% nonfat milk/TBS-T for 1 hour at room temperature. Western blotting was performed using the aforementioned primary antibodies, secondary anti-mouse or anti-rabbit IgG antibody-HRP conjugates (GE Healthcare), and enhanced chemiluminescence (SuperSignal West Pico or SuperSignal West Femto Pierce, Nepean, ON, Canada).

Measurement of Inositol Phosphate Formation. HEK 293 cells were transiently transfected with the cDNAs as described in the figure legends. Forty-eight-hour post-transfection cells were incubated overnight in inositol- and glutamine-free DMEM with 100 μCi/ml *myo*-[^{3}H]-inositol. For all experiments, cells were incubated for 1 hour in warm Hanks' balanced salt solution (HBSS) (116 mM NaCl, 20 mM HEPES, 11 mM glucose, 5 mM NaHCO3, 4.7 mM KCl, 2.5 mM CaCl2, 1.2 mM MgSO4, 1.2 mM KH2PO4, pH 7.4) and were then incubated with 10 mM LiCl alone for 10 minutes followed by 30 μM quisqualate in LiCl for 30 minutes. Cells were placed on ice, and the reaction was stopped with 500 μl of perchloric acid and neutralized with 400 μl of 0.72 M KOH, 0.6 M $KHCO_3$. Total cellular [^{3}H]-inositol incorporation was determined in 50 μl of cell lysate. Total IP was purified by anion exchange chromatography using Dowex 1-X8 (formate form) 200–400 mesh anion exchange resin, and [^{3}H]-inositol phosphate formation was determined by liquid scintillation using a Beckman LS 6500 scintillation system (Mississauga, ON, Canada).

Confocal Microscopy. Confocal microscopy was performed using a Zeiss LSM-510 META laser scanning confocal microscope equipped with a Zeiss 63×, 1.4 numerical aperture, oil immersion lens (North York, ON, Canada). For live cell imaging, HEK 293 cells expressing FLAG-mGluR1a constructs were serum starved for 1 hour at 37°C in HBSS. HEK 293 cells were prelabeled with Zenon Alexa Fluor 568-conjugated with anti-FLAG polyclonal rabbit antibody. Cells were then either kept on ice or stimulated with 30 μM quisqualate for 30 minutes at 37°C. For fixed cell imaging, cells were washed three times at room-temperature phosphate-buffered saline, fixed for 10 minutes at room temperature with periodate-lysine-paraformaldehyde fixative, followed by 10 minutes of permeablilization with 0.01% Triton X-100. Cells were blocked with 3% normal donkey serum (Jackson ImmunoResearch) and labeled with rabbit anti-FLAG polyclonal rabbit antibody followed by donkey anti-rabbit Alexa Fluor 488. ER was labeled with green fluorescence protein (GFP)–fused lysine-aspartate-glutamate-leucine (KDEL-GFP) ER retention sequence. Colocalization studies were performed using dual excitation (488, 543 nm) and emission (bandpass 505–530 nm and long-pass 560 nm for Alexa Fluor 488 and 568, respectively) filter sets.

Flow Cytometry. HEK 293 cells were transiently transfected with the cDNAs described in the figure legends. Forty-eight-hour post-transfection cells were placed on ice and washed in ice-cold HBSS. FLAG-tagged mGluR1α constructs were labeled with primary rabbit anti-FLAG antibody (1:500), followed by secondary goat anti-rabbit AlexaFluor-488 antibody (1:500). Cells were incubated for 10 minutes in 5 mM EDTA, gently removed from the dish by pipetting, and fixed in 3.6% formaldehyde. Cell surface mean fluorescence was assessed by flow cytometry.

Statistical Analysis. Densitometric data were normalized first for protein expression, and the maximum value was set to 100, with all other values displayed as percentage thereof. One-way analysis of variance test was performed to determine significance, followed by a post-hoc Tukey multiple comparison test or Bonferroni's multiple comparisons test to determine which means were significantly different ($P < 0.05$) from one another.

Results

Mutations in the Cysteine-Rich Domain Alter Receptor Cell Surface Expression. Eight somatic variants in *GRM1* were previously identified in variety of tumor types with four localized to the amino-terminal domain of mGluR1a (D44E, A168V, R375G, and G396V); three localized to the mGluR,1a second intracellular loop (R684C, G688V and R696W); and one localized to the Homer binding motif (P1148L) (Fig. 1) (Sjoblom et al., 2006; Wood et al., 2007; Parsons et al., 2008; Kan et al., 2010). We first examined whether the cell surface expression of FLAG-mGluR1a was affected by each of the mutations introduced into the coding sequence of mGluR1a. None of the somatic mutations resulted in an overall change in cellular protein expression as determined by Western blot (Fig. 2A). Densitometric analysis revealed no differences in total expression of each of the Flag-mGluR1a variants when compared with wild-type FLAG-mGluR1a expression (Fig. 2B). However, FLAG-mGluR1a-R375G and -G396V exhibited reduced cell surface expression as assessed by flow cytometry, with cell surface expression reduced to 39.7 ± 5.1% and 43.4 ± 3.2% of wild-type mGluR1a control transfected cells, respectively (Fig. 2C). The reduction in cell surface FLAG-mGluR1a-R375G and -G396V expression was associated with an increased retention of both receptor mutants in the ER as demonstrated by increased colocalization with the ER marker construct KDEL-GFP (Fig. 3, D and E). Thus, both the R375G and G396V mutations result in a significant reduction of mGluR1a expression at the cell surface as a consequence of ER retention.

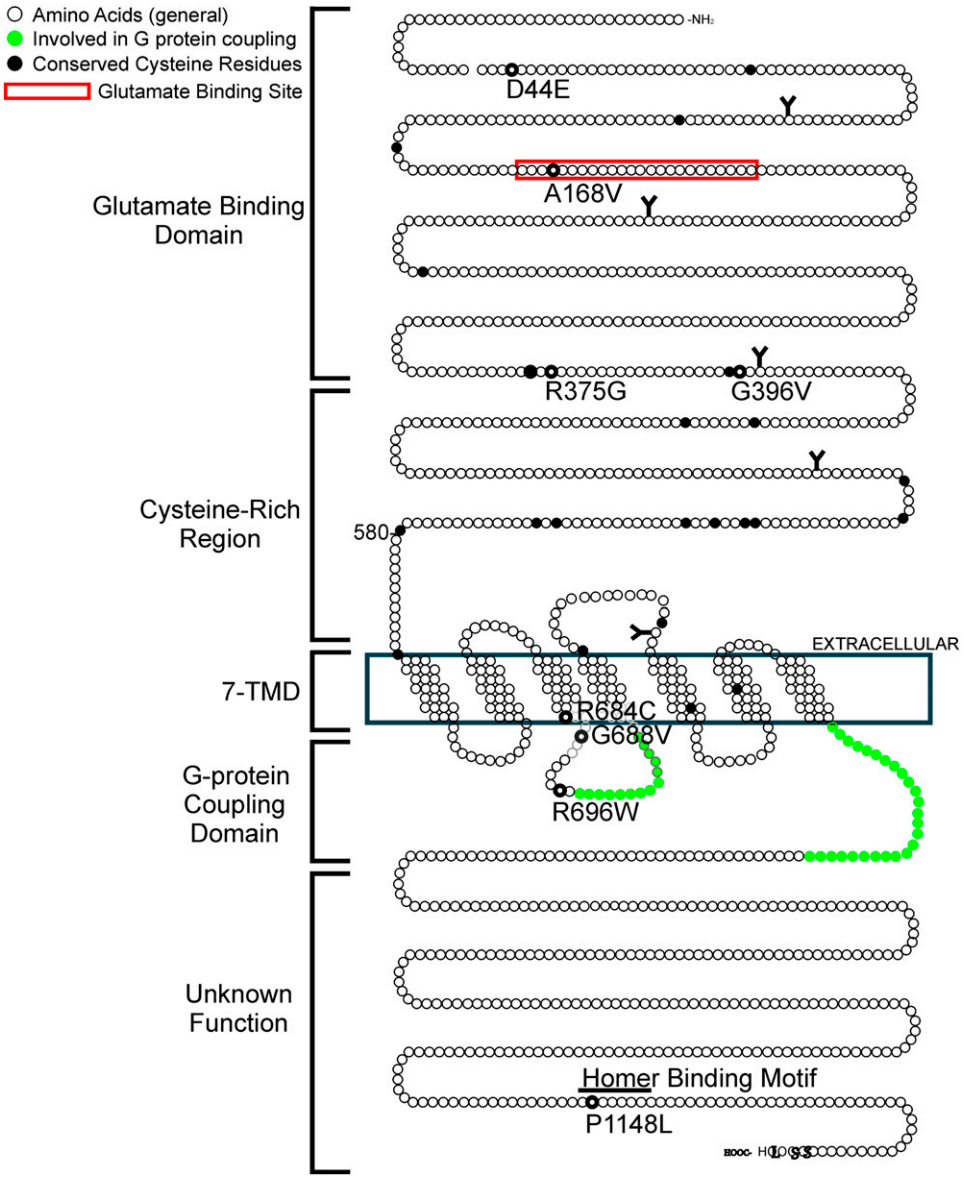

Fig. 1. Eight somatic variants in *GRM1* (mGluR1a) found in cancer. The locations of eight somatic mutations have been identified within the coding sequence for mGluR1a, including A168V, a mutation in the orthosteric glutamate binding region identified in lung adenocarcinoma; two mGluR1a variants in the cysteine-rich region, R375G (identified in squamous cell carcinoma) and G396V (identified in lung adenocarcinoma); three variants in the second intracellular loop, including the glioblastoma mutation (R684C), the squamous cell carcinoma mutation (G688V), and the colorectal cancer R696W mutation located close to the putative PKC phosphorylation site T695A. An additional colorectal cancer mutation is located within the Homer binding region in the carboxyl-terminal region of mGluR1a (P1148L).

Mutations in the Amino-Terminus Exhibit Altered Basal and Agonist-Activated Activity. Group I mGluRs activate both IP and ERK signal transduction cascades and exhibit high basal activity (Dale et al., 2000). Interestingly, three of the four amino-terminal mGluR1a variants we examined (A168V, R375G, G396V) showed significantly reduced basal IP formation (in the absence of agonist) compared with wild type, and FLAG-mGluR1a-R375G exhibited basal IP formation that was indistinguishable from nontransfected cells (Fig. 4A). Quisqualate-mediated activation of FLAG-mGluR1a-A168V (a variant located within the glutamate binding region) resulted in a 63 ± 17% increase in IP formation above basal compared with control FLAG-mGluR1a transfected cells (Fig. 4B). Quisqualate-stimulated FLAG-mGluR1a-R375G IP formation above basal was comparable to FLAG-mGluR1a wild type transfected cells, despite reduced cell surface expression. However, when total quisqualate-stimulated mGluR1a variant IP formation was assessed, total FLAG-mGluR1a-A168V-stimulated IP formation was indistinguishable from Flag-mGluR1a, whereas total FLAG-mGluR1a-R375G-mediated IP formation was impaired (Fig. 4C). Interestingly, in response to 100 μM glutamate treatment, FLAG-mGluR1a-R375G-mediated IP formation above basal IP levels was reduced to 29 ± 4% of cells transfected with FLAG-mGluR1a (Fig. 4D). Glutamate-mediated activation of FLAG-mGluR1a-A168V also resulted in increased IP formation above basal compared with control FLAG-mGluR1a transfected cells (Fig. 4D). In response to glutamate, the

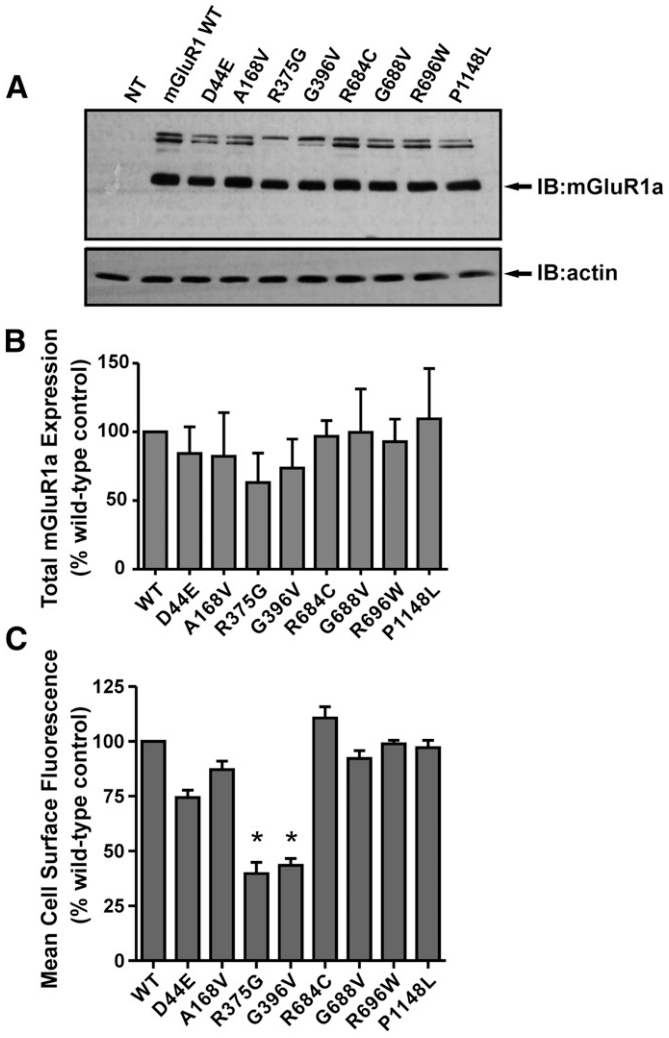

Fig. 2. Cell surface expression and intracellular localization of mGluR1a variants. (A) Representative Western blot of HEK 293 cells transfected with 1-3.5 μg of plasmid cDNA encoding FLAG-tagged mGluR1a SNV constructs. (B) Shown is the densitometric analysis of autoradiographs showing the mean ± S.E.M. of five independent experiments examining the total cellular expression of wild-type FLAG-mGluR1a and the FLAG-mGluR1a variants. (C) HEK 293 cells transfected with 2 μg of plasmid cDNA encoding FLAG-tagged mGluR1a SNV constructs were immunolabeled, and cell surface mean fluorescence was assessed by flow cytometry. Data were normalized for total cell surface wild-type mGluR1a protein expression. Data represents the mean ± S.D. of four independent experiments. *$P < 0.05$ compared with wild-type mGluR1a expression.

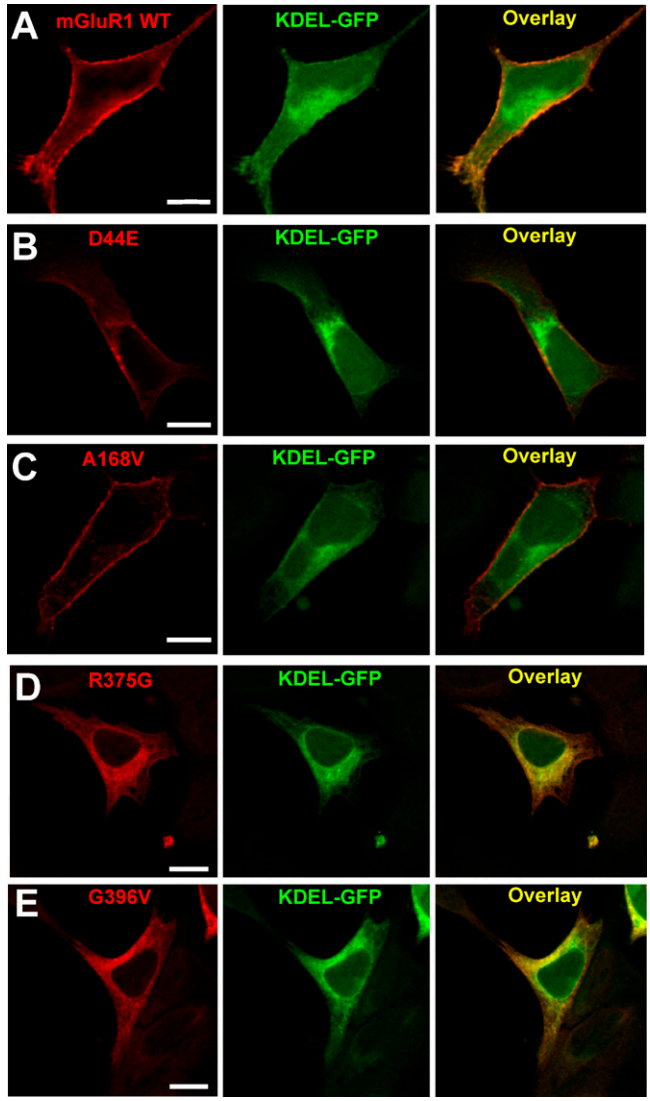

Fig. 3. mGluR1a variants localize to endoplasmic reticulum. Representative confocal micrographs illustrating receptor intracellular localization (red) and colocalization with the endoplasmic reticulum marker GFP-KDEL (green). HEK 293 cells transfected with 1-3.5 μg of plasmid cDNA encoding either **(A)** FLAG-tagged mGluR1a, (B) FLAG-tagged mGluR1a-D44E, (C) FLAG-tagged mGluR1a-A168V, (D) FLAG-tagged mGluR1a-R375G, or (E) FLAG-tagged mGluR1a-G396V constructs along with 1 μg of plasmid cDNA encoding KDEL-GFP were fixed and immunolabeled for total cellular complement of receptor. Images are representative of three independent experiments. Bars represent 10 μm.

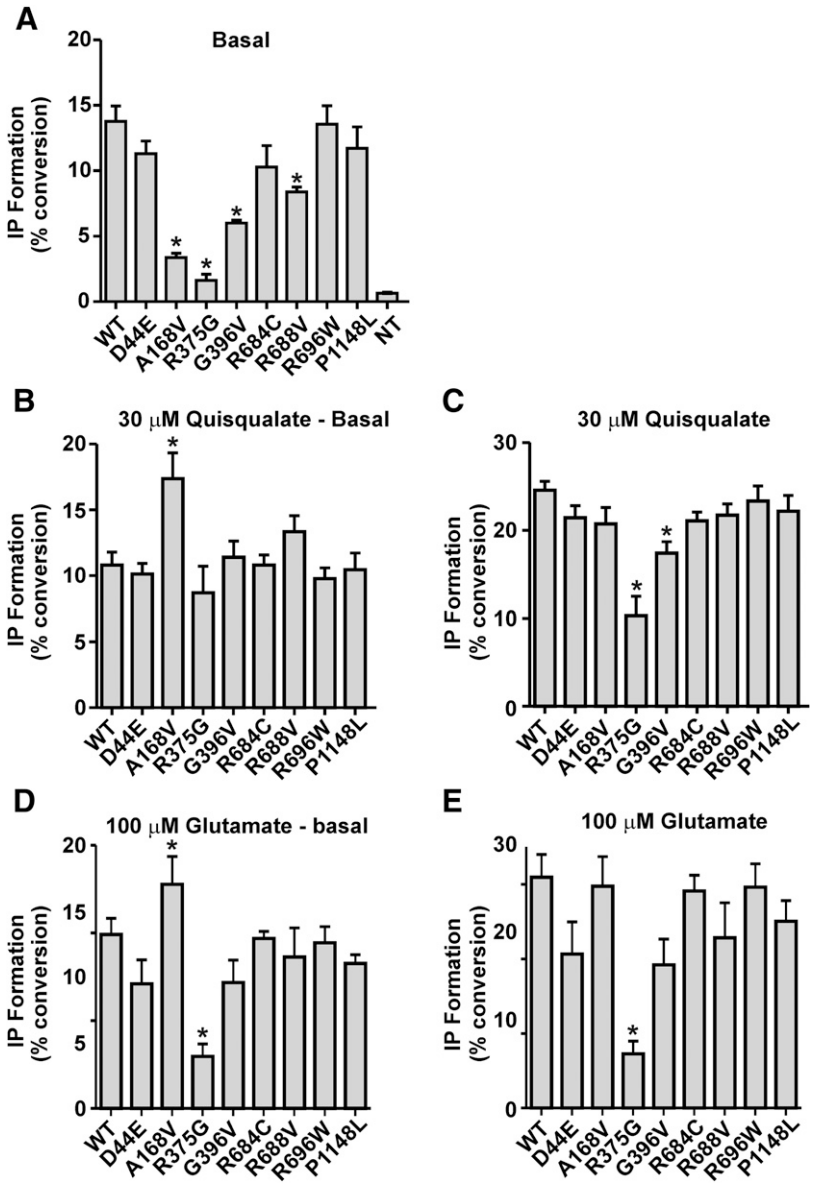

Fig. 4. Mutations in mGluR1a alter basal and agonist-activated inositol phosphate formation. HEK 293 cells transiently transfected with 1-3.5 μg of plasmid cDNA encoding FLAG-tagged mGluR1a SNV constructs. **(A)** Basal IP formation was determined in cells that were labeled overnight with *myo*-(^{3}H)inositol in glutamine-free DMEM and incubated for 10 minutes with 10 mM LiCl. (B) Increase in IP formation above basal after agonist stimulation with 30 μM quisqualate for 30 minutes. (C) Total IP formation (basal + agonist stimulated) after agonist stimulation with 30 μM quisqualate. (D) Increase in IP formation above basal after agonist stimulation with 100 μM glutamate for 30 minutes. (E) Total IP formation (basal + agonist stimulated) after agonist stimulation with 100 μM glutamate. Data were normalized for mGluR1 protein expression at the cell surface as determined by flow cytometry and represent the mean ± S.D. of four independent experiments. *$P < 0.05$ compared with wild-type mGluR1a IP formation.

maximal capacity of FLAG-mGluR1a-A168V to activate G protein signaling was not different from wild-type FLAG-mGluR1a, whereas FLAG-mGluR1a-R375G signaling was impaired (Fig. 4E). Therefore, activation of this mutant by glutamate and quisqualate resulted in divergent signaling patterns.

To evaluate further how mutations in the amino terminus affect agonist activation, we looked at dose-dependent receptor activation in response to increasing concentrations of quisqualate. The FLAG-mGluR1a-A168V mutant did not exhibit an alteration in the EC_{50} for quisqualate-mediated IP formation but significantly increased the E_{MAX} for quisqualate-stimulated IP formation (Fig. 5). Interestingly, although FLAG-mGluR1a-R375G maximal response to quisqualate was unchanged from wild type, this mutant produced a significantly right-shifted EC_{50} of 3.1×10^{-6} M compared with wild-type EC_{50} of 2.3×10^{-8} M (Fig. 5). Therefore, although FLAG-mGluR1a-R375G couples effectively to the cognate G protein to trigger signal transduction, this mutant exhibits decreased affinity for the ligand compared with wild-type receptor.

R375G Displays Functional Selectivity toward ERK1/2. To examine whether the mGluR1a cancer mutations also affected other mGluR1a-activated cell signaling pathways, we examined whether the variants influenced the ability of mGluR1a to stimulate ERK1/2 phosphorylation in HEK 293 cells. Similar to what we found for IP formation, all four amino-terminal mutations, as well as the G688V mutant, exhibited decreased basal ERK1/2 phosphorylation but still displayed a statistically significant increase in IP formation in response to quisqualate treatment (Fig. 6A). Interestingly, although FLAG-mGluR1a-R375G demonstrated decreased basal ERK1/2 phosphorylation, quisqualate treatment of FLAG-mGluR1a-R375G expressing cells resulted in significantly increased ERK1/2 phosphorylation after 1, 5, and 15 minutes of agonist stimulation compared with wild-type FLAG-mGluR1a (Fig. 6B). In contrast, ERK1/2 phosphorylation in response to the activation of either FLAG-mGluR1a-R696W or -P1148L was significantly reduced compared with wild-type FLAG-mGluR1a. Therefore, the R375G mutant appeared to be biased toward activation of the ERK1/2 pathway, whereas the R696W and P1148L were biased

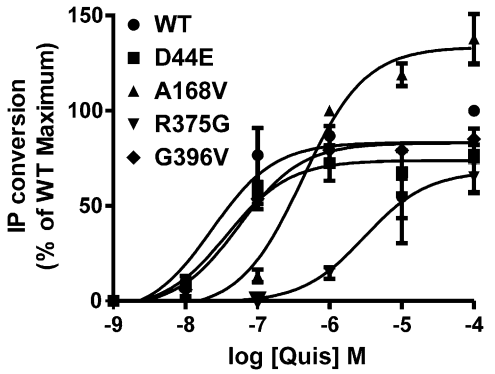

Fig. 5. Mutations in mGluR1a alter dose-dependent quisqualate inositol phosphate formation. HEK 293 cells transiently transfected with 2–3.5 μg of plasmid cDNA encoding FLAG-tagged mGluR1a amino-terminal mutant constructs. Increases in IP formation above basal was determined in cells labeled overnight with *myo*-(^{3}H)inositol in glutamine-free DMEM and incubated for 10 minutes with 10 mM LiCl followed by 30 minutes in 10 mM LiCl with increasing concentrations of quisqualate. Data were normalized for protein expression and represent the mean ± S.D. of three independent experiments.

for G protein-mediated signaling. To determine whether this altered ERK1/2 activity resulted from differential association with proteins known to mediate mGluR1a activation of ERK, we performed coimmunoprecipitation experiments with the mGluR1a effector Pyk2. When normalized for HA-Pyk2 protein expression, none of the mutants studied exhibited altered association with HA-Pyk2 compared with wild-type FLAG-mGluR1a (Fig. 7). Therefore, the altered downstream activation of ERK1/2 by several of the mutants studied is not mediated by altered receptor association with Pyk2.

GRK2 Binding to mGluR1a SNV Mutants. Several of the identified mGluR1a alterations are localized to the second intracellular loop domain of the receptor, including R684C, G688V, and R696W, a domain that is important for GRK2 binding and phosphorylation-independent desensitization of the receptor (Pin et al., 1994; Dhami et al., 2004). To examine whether GRK2-mediated IP desensitization was altered, we compared the ability of GRK2 to desensitize cells expressing wild-type mGluR1a versus the mGluR1a variants. Surprisingly, we observed no alterations in IP formation between

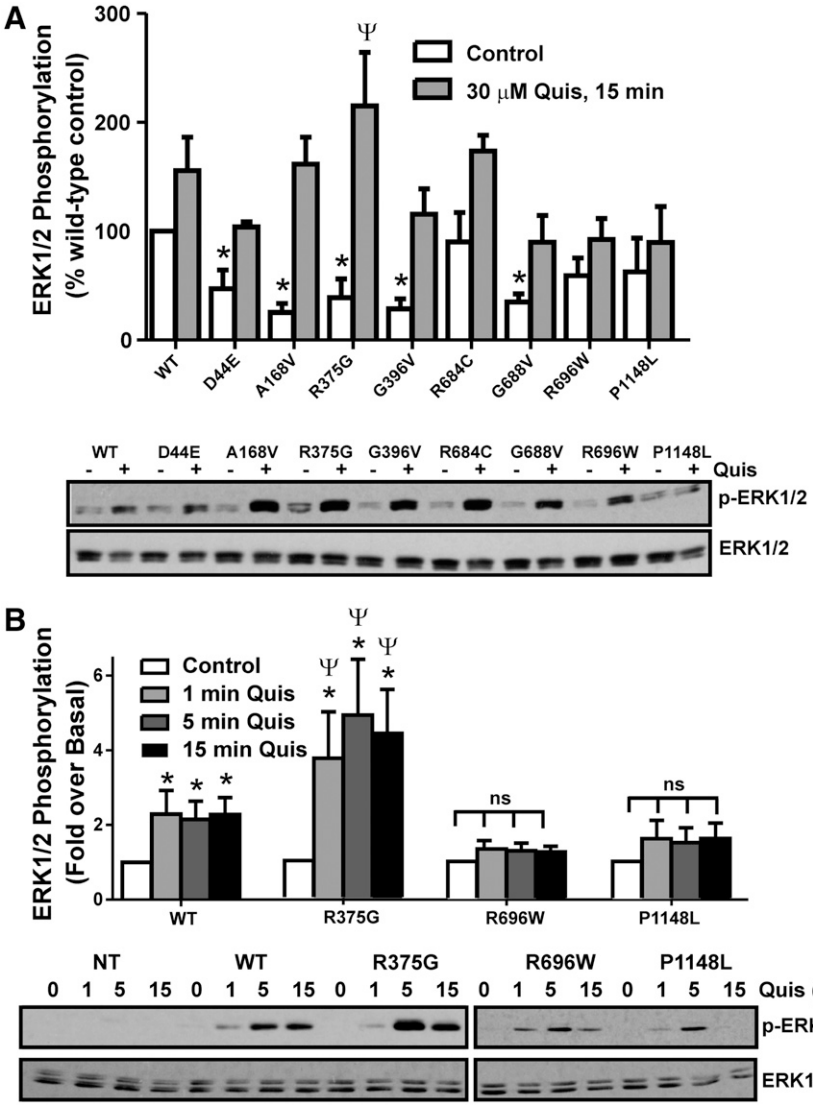

Fig. 6. Mutations in mGluR1a alter agonist-stimulated ERK1/2 activation. (A) HEK 293 cells were transiently transfected with 2 μg of plasmid cDNA encoding FLAG-mGluR1a SNV constructs. Forty-eight hours post-transfection, cells were serum starved overnight in glutamine-free DMEM and stimulated for 15 minutes with 30 μM quisqualate. Shown are representative immunoblots for phosphorylated and total p42/44 (ERK1/2). The data were normalized for protein expression and plotted as the percent change in ERK1/2 phosphorylation compared with wild-type (WT) mGluR1a ERK1/2 phosphorylation on the same immunoblot in the absence of agonist treatment (control). The data represent the mean ± S.D. of five independent experiments $^*P < 0.05$ compared with basal ERK1/2 phosphorylation. $\Psi P < 0.05$ compared with agonist-stimulated wild-type mGluR1a ERK1/2 phosphorylation. (B) HEK 293 cells were transiently transfected with 2 μg of plasmid cDNA encoding FLAG-mGluR1a, FLAG-mGluR1a-R696W, FLAG-mGluR1a-P1148, or FLAG-mGluR1a-R375G. Forty-eight hours post-transfection, cells were serum starved overnight in glutamine-free DMEM and stimulated for 0, 1, 5, or 15 minutes with 30 μM quisqualate. Shown are representative immunoblots for phosphorylated and total p42/44 (ERK1/2). The data represent the mean ± S.D. of five independent experiments. $^*P < 0.05$ compared with basal ERK1/2 phosphorylation. ns, not significant, $\Psi P < 0.05$ compared with agonist-stimulated wild type mGluR1a ERK1/2 phosphorylation.

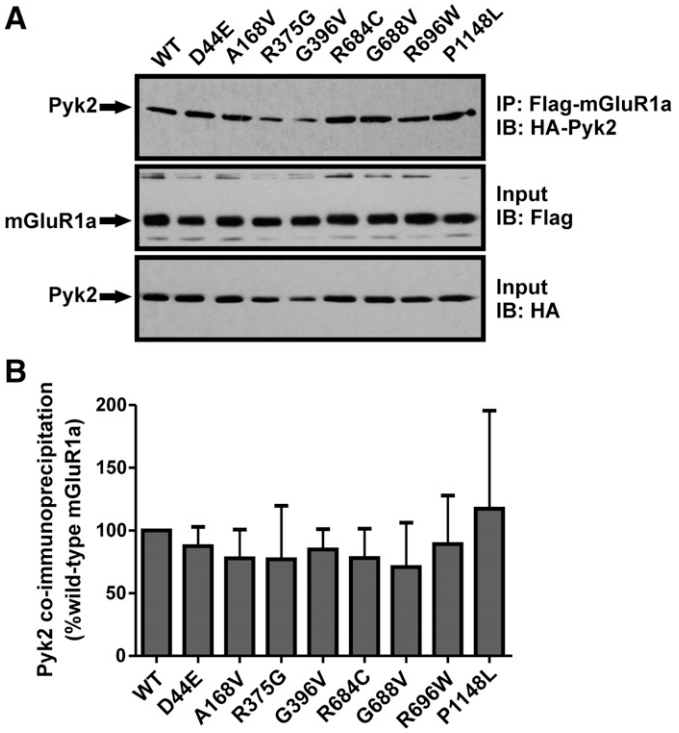

Fig. 7. mGluR1a mutants maintain association with Pyk2. (A) HEK 293 cells were transiently transfected with 2–3.5 μg of plasmid cDNA encoding FLAG-tagged mGluR1a SNV constructs along with 1 μg of plasmid cDNA encoding HA-Pyk2. Forty-eight hours post-transfection, the FLAG-mGluR1a SNV constructs were immunoprecipitated with FLAG antibody and immunoprecipitated protein resolved by SDS-PAGE and immunoblotted with FLAG and HA antibodies. (B) Shown is the densitometric analysis of autoradiographs showing the mean ± S.E.M. of four independent experiments examining the coimmunoprecipitation of HA-Pyk2 with the FLAG-mGluR1a SNV constructs. The data are normalized for FLAG-mGluR1a and HA-Pyk2 protein expression and presented as a percentage of HA-Pyk2 co-immunoprecipitation with wild-type mGluR1a.

cells expressing wild-type mGluR1a versus the cancer variants (Fig. 8A), and this was further supported by comparable association between mGluR1a wild type and variants with GRK2 in coimmunoprecipitation studies (Fig. 8B). Therefore, although there are mutations in a region critical for association and desensitization of the receptor by GRK2, we observed neither changes in GRK2-mediated IP desensitization (Fig. 8A) nor decreases in GRK2 interaction between the mGluR1a variants (Fig. 8C).

Attenuated Homer Binding to FLAG-mGluR1a P1148L. The carboxyl-terminus mGluR1a encodes a Homer binding motif, and the association of Homers with mGluR1a was shown to modulate both the subcellular localization and signaling of mGluR1a (Brakeman et al., 1997; Roche et al., 1999; Ango et al., 2002; Kammermeier, 2008). The introduction of the P1148L variant into the C-tail of FLAG-mGluR1a did not affect IP formation in response to agonist activation of the receptor (Fig. 4), but it diminished agonist-stimulated ERK1/2 phosphorylation and resulted in a loss of Homer1b binding to the receptor as determined by coimmunoprecipitation (Fig. 6B and Fig. 9). Homer1b binding to FLAG-mGluR1a-G396V, which was retained in the ER, was also reduced (Fig. 9). The P1148L mutation also resulted in altered subcellular localization of mGluR1a to membrane ruffles in HEK 293 and increased filopodia formation in HEK 293 cells

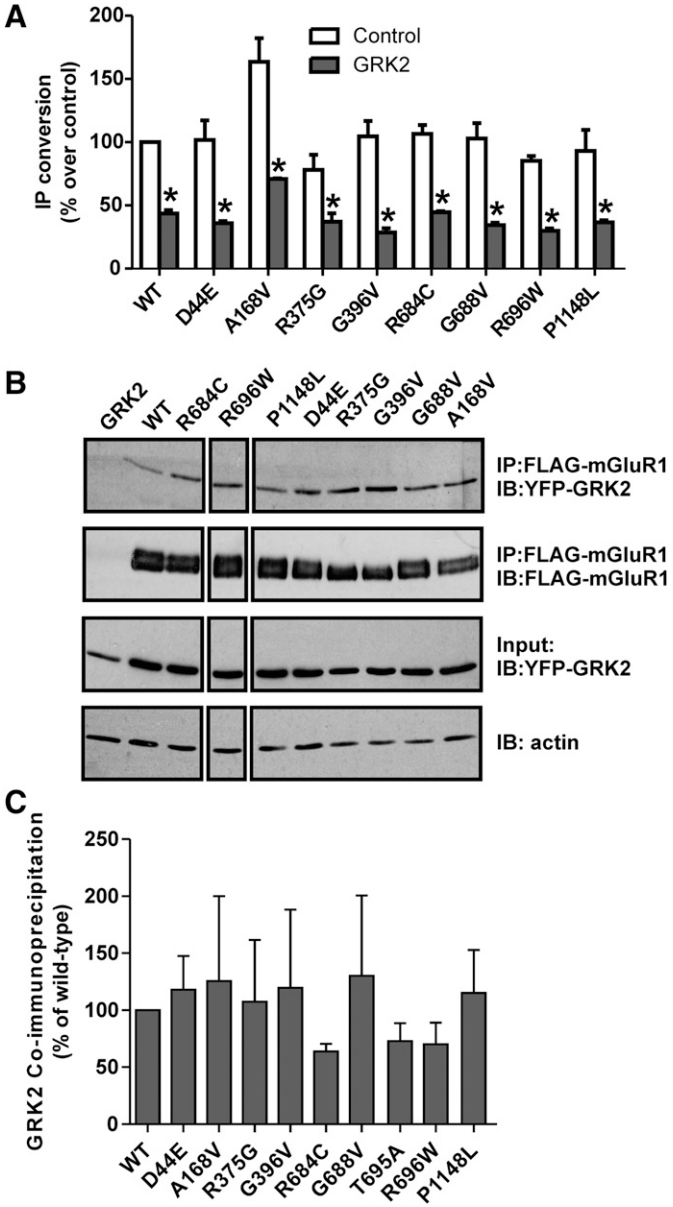

Fig. 8. Effect of mGluR1a variants on GRK2 binding and receptor desensitization. (A) HEK 293 cells were transiently transfected with 2 μg of plasmid cDNA encoding FLAG-tagged mGluR1a SNV constructs along with 1 μg of plasmid cDNA encoding either empty vector or HA-GRK2. Cells were labeled overnight with *myo*-(^{3}H)inositol in glutamine-free DMEM, incubated for 10 minutes with 10 mM LiCl and then treated with 30 μM quisqualate for 30 minutes. Data are expressed as the increase in IP formation above basal after agonist stimulation with 30 μM quisqualate for 30 minutes. Data were normalized for mGluR1 protein expression at the cell surface as determined by flow cytometry and represent mean ± S.D. of three independent experiments. $^*P < 0.05$ compared with agonist-stimulated IP formation in the absence of GRK2 overexpression. (B) Forty-eight hours post-transfection, the FLAG-mGluR1a SNV constructs were immunoprecipitated with FLAG antibody and immunoprecipitated protein resolved by SDS-PAGE and immunoblotted with FLAG, GFP (YFP; yellow fluorescent protein), and actin antibodies. The blots have been cut to remove lanes that correspond to FLAG-mGluR1a mutants examined that did not correspond to mGluR1a SNVs and were not pursued functionally. (C) Shown is the densitometric analysis of autoradiographs showing the mean ± S.E.M. of four independent experiments examining the coimmunoprecipitation of YFP-GRK2 with the FLAG-mGluR1a SNV constructs. The data are normalized for FLAG-mGluR1a and YFP-GRK2 protein expression and presented as a percentage of YFP-GRK2 coimmunoprecipitation with wild-type mGluR1a.

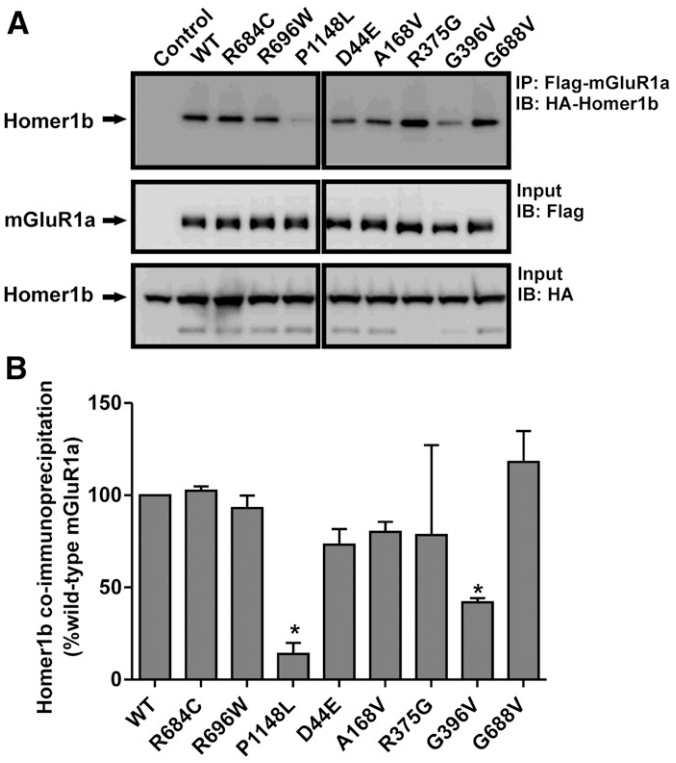

Fig. 9. mGluR1a P1148L is deficient in Homer1b binding. (A) HEK 293 cells were transiently transfected with 2 μg of plasmid cDNA encoding FLAG-tagged mGluR1a SNV constructs along with 1 μg of plasmid cDNA encoding HA-Homer1b. Forty-eight hours post-transfection, the FLAG-mGluR1a SNV constructs were immunoprecipitated with FLAG antibody and immunoprecipitated protein resolved by SDS-PAGE and immunoblotted with FLAG, HA, and actin antibodies. The blots were cut to remove lanes that correspond to FLAG-mGluR1a mutants examined that did not correspond to mGluR1a SNVs and were not pursued functionally. (B) Densitometric analysis of autoradiographs showing the mean ± S.D. of four independent experiments examining the coimmunoprecipitation of HA-Homer1b with the FLAG-mGluR1a SNV constructs. The data are normalized to HA-Homer1b coimmunoprecipitation with wild-type mGluR1a. *$P < 0.05$ compared with wild-type FLAG-mGluR1a.

(Fig. 10A-C) and NIH 3TC cells (data not shown). On observing the increased filopodia in HEK 293 cells, we evaluated this in NIH 3T3 cells, a cell type with more well characterized morphologic changes that are easily quantifiable. As seen in HEK 293 cells, FLAG-mGluR1a P1148L expression in NIH 3T3 cells also resulted in significantly higher filipodia formation, an effect that was not observed for the wild-type receptor (Fig. 10D). Therefore, a loss of homer binding results in increased filipodia formation that might be associated with alterations in cellular migration in an appropriate cancer cell line.

Discussion

In the present study, we characterized the intracellular localization, signaling, and association with regulatory molecules and cellular morphology of eight previously unstudied somatic variants in *GRM1* (Sjoblom et al., 2006; Parsons et al., 2008; Kan et al., 2010). Group I mGluRs exhibit significant basal G protein activation (Dale et al., 2000). However, three amino-terminal mGluR1a variants—A168V, R375G, and G396V—as well as one second intracellular loop variant (G688V), exhibited a loss of basal activity in HEK 293 cells. The reduction in basal activity for the amino-terminal mGluR1a mutations may be the consequence of altered affinity for glutamate that may be released from the HEK 293 cells to feedback on the receptor. However, inconsistent with this notion is the observation that the mGluR1a-A168V mutant exhibits increased activation of IP formation in response to agonist treatment. The intracellular loop mutation G688V also resulted in decreased basal mGluR1a activity without affecting agonist-stimulated responses. The rationale for this observed reduction in basal activity of the mGluR1a-G688V variant remains to be determined.

It is well established that mGluRs activate downstream mitogenic pathways, such as the ERK1/2 signaling cascade, that contribute to alterations in cell proliferation (Rozengurt, 2007). Group I mGluRs activate ERK1/2 in both calcium-dependent and -independent manners, the latter involving G$\beta\gamma$ and non–receptor tyrosine kinases such as Src and Pyk2, as well as Homer (Mao et al., 2005; Nicodemo et al., 2010). We have identified three mGluR1a mutants with altered ERK1/2 activation. The R696W and P1148L mutations result in a loss of mGluR1a agonist–stimulated ERK1/2 phosphorylation without affecting G protein-coupling required for IP formation. The R375G mutation significantly impairs mGluR1a-mediated IP formation in response to glutamate treatment and results in an overall reduction in the ability of mGluR1a to stimulate IP formation in response to quisqualate treatment. However, despite the reduced expression of the R375G mutant at the cell surface and decreased overall G protein coupling, the mutant exhibits enhanced coupling to the activation of ERK1/2 compared with the wild-type mGluR1a, potentially through its ability to signaling via Pyk2. Taken together, these observations suggest that the R375G mutation localized to the amino-terminal domain of mGluR1a may bias receptor signaling via the ERK1/2 pathway, which may be relevant to a cancer phenotype.

The overexpression of mGluR1 in melanocytes promotes development and growth of melanoma (Pollock et al., 2003; Ohtani et al., 2008; Martino et al., 2012), and, more recently, the molecular mechanisms supporting mGluR1-promoted melanoma formation, have been elucidated. Although it appears that activation of numerous mGluR1-promoted signaling pathways is required for melanoma development, it is activation of the ERK pathway by mGluR1 that plays a key role in melanoma growth (Abdel-Daim et al., 2010); as such, mGluR1 R375G, which biases receptor signaling to ERK, may promote tumor progression through increased cancer growth.

Receptor modulation by regulatory proteins such as GRK2 represents a major mechanism controlling the magnitude and duration of GPCR signal transduction. GRK2-mediated attenuation of mGluR1a signaling occurs as the consequence of the concomitant association of the kinase with the second intracellular loop domain of the receptor and Gαq (Dhami et al., 2004, 2005; Dhami and Ferguson, 2006; Ferguson, 2007). We investigated the effect of three intracellular loop 2 SNVs on the association of GRK2 with mGluR1a. We found that all the mutations retained GRK2 association. In line with this, GRK2 overexpression resulted in normal attenuation of G protein signaling in response to the activation of all the mGluR1a mutants. Interestingly, we found that ERK1/2 activation in response to activation of mGluR1a-R696W is lost, suggesting that this residue may contribute to the

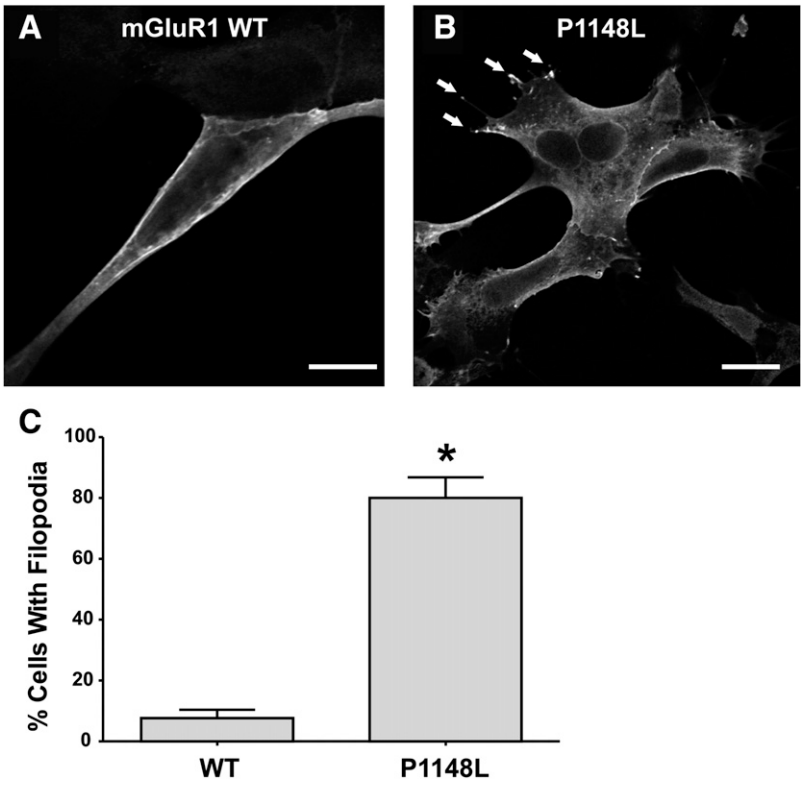

Fig. 10. Homer binding mutant mGluR1a P1148L promotes filopodia formation. Representative confocal micrographs illustrating receptor localization and cell morphology in HEK 293 cells transiently transfected with 2 μg of plasmid cDNA encoding either (A) wild-type FLAG-mGluR1a or (B) FLAG-mGluR1a-P1148L. Cells were fixed and immunolableled for total cellular mGluR1a expression. Images are representative of three independent experiments. Bars represent 10 μm. (C) Graph scoring the number of filopodia per cell. NIH 3T3 cells transiently transfected with 2 μg of plasmid cDNA encoding either FLAG-mGluR1a wild-type or FLAG-mGluR1a-P1148L were fixed and immunolabeled for total cellular complement of the receptor, and the number of filopodia were counted per field of view by a blinded observer. $^*P < 0.05$. Filopodia were defined as cellular protrusions. Data represent the mean ± S.D. of 300 random cells, total 100 from three independent experiments.

regulation of ERK1/2 signaling by the receptor. Our previous studies have shown that Pyk2 binds to the second intracellular loop domain of mGluR1a and may directly contribute to the activation of ERK1/2 (Nicodemo et al., 2010). However, here we find that none of the mutants studied show altered association with Pyk2.

Of the many regulatory proteins that interact with Group I mGluRs, the Homer family of proteins are predominantly featured as they are synaptically localized and couple Group I mGluRs to the activation of a variety of ion channels at the synapse (Roche et al., 1999; Tadokoro et al., 1999; Ango et al., 2002). Here we show that the mGluR1a variant P1148L does not associate with Homer1b, is uncoupled from the activation of ERK1/2, and causes enhanced filopodia formation in HEK 293 cells. The loss of agonist-stimulated ERK1/2 phosphorylation by the mGluR1a-P1148L mutant is consistent with recent reports that Homer1a may contribute in part to the coupling of mGluR1a to the activation of ERK1/2 (Mao et al., 2005). The mechanism by which the P1148L mutation leads to increased filopodia formation is unclear, but Homer proteins may contribute to the regulation of actin dynamics through their interactions with the actin cytoskeletal regulatory proteins Cdc42 and Drebin (Shiraishi-Yamaguchi et al., 2009).

Several factors are involved in tumor progression and metastasis, including altered cell motility and promotion of angiogenesis. Numerous GPCRs have been shown to drive cell migration and vascular remodelling through both direct and indirect mechanism, including PAR and AT1R. Recently, CCK2R cancer variants were shown to alter cellular morphology (i.e., filopodia and lamellipodia formation), increase cell migration, and promote angiogenesis, leading to enhanced tumorigenesis (Willard et al., 2012). Ectopic overexpression of mGluR1 in both melanocytes and epithelial cells promotes formation of robust tumors, and the malignancy of these tumors is evident by increased angiogenesis and invasion to muscle and intestine (Shin et al., 2008; Martino et al., 2012). Thus, mGluR1 P1148L, which increases filopodia formation, may stimulate tumorigenesis through changes in cell behavior that promote a malignant phenotype.

In conclusion, in this study, we characterized the signaling and intracellular localization of eight somatic mutations in *GRM1* identified in genome-wide screens of various cancer types. We identified two mutations involved in plasma membrane targeting, as well as several mutations differentially affecting IP formation and MAPK signaling of this receptor. For example, we demonstrate that the R375G SNV preferentially couples to ERK1/2 activation while exhibiting decreased basal and glutamate-activated IP production. Additionally, the A168V SNV displays decreased basal and increased agonist-mediated IP formation. These alterations in the mGluR1a activity may contribute, at least in part, to the phenotype of the cancer in which they were identified. This study sheds new light on the functionality of different regions of the receptor, as well as further defining the residues involved in mGluR1a signaling and the role of mGluR1a signaling in pathologies, and may provide an exciting opportunity for developing new mGluR1a-targeted treatments.

Acknowledgments

The authors thank James Starling and Christoph Reinhard for project support; Mel Baez, Beverly Heinz, Shaoyou Chu, Christopher Moxham, Shaillay Kumar Dogra, Mohamed Roohul Ameen, Jiahang Song, Dong Liang Guo, Marcio Chedid, Andrew Capen, Yue-wei Qian, Francis Willard, David Clawson, and Suzie Chen for experimental assistance and project guidance.

Authorship Contributions

Participated in research design: Esseltine, Willard, Lajiness, Barber, Ferguson.

Conducted experiments: Esseltine, Willard, Wulur.

Contributed new reagents or analytic tools: Esseltine, Willard, Lajiness, Barber, Ferguson.

Performed data analysis: Esseltine, Willard, Wulur.

Wrote or contributed to the writing of the manuscript: Esseltine, Willard, Barber, Ferguson.

References

Abdel-Daim M, Funasaka Y, Komoto M, Nakagawa Y, Yanagita E, and Nishigori C (2010) Pharmacogenomics of metabotropic glutamate receptor subtype 1 and in vivo malignant melanoma formation. *J Dermatol* **37**:635–646.

Ango F, Robbe D, Tu JC, Xiao B, Worley PF, Pin JP, Bockaert J, and Fagni L (2002) Homer-dependent cell surface expression of metabotropic glutamate receptor type 5 in neurons. *Mol Cell Neurosci* **20**:323–329.

Brakeman PR, Lanahan AA, O'Brien R, Roche K, Barnes CA, Huganir RL, and Worley PF (1997) Homer: a protein that selectively binds metabotropic glutamate receptors. *Nature* **386**:284–288.

Cancer Genome Atlas Research Network (2008) Comprehensive genomic characterization defines human glioblastoma genes and core pathways. *Nature* **455**:1061–1068.

Cancer Genome Atlast Research Network (2011) Integrated genomic analyses of ovarian carcinoma. *Nature* **474**:609–615.

Choi KY, Chang K, Pickel JM, Badger JD, 2nd, and Roche KW (2011) Expression of the metabotropic glutamate receptor 5 (mGluR5) induces melanoma in transgenic mice. *Proc Natl Acad Sci USA* **108**:15219–15224.

Conn PJ and Pin JP (1997) Pharmacology and functions of metabotropic glutamate receptors. *Annu Rev Pharmacol Toxicol* **37**:205–237.

Dale LB, Babwah AV, Bhattacharya M, Kelvin DJ, and Ferguson SSG (2001) Spatial-temporal patterning of metabotropic glutamate receptor-mediated inositol 1,4,5-triphosphate, calcium, and protein kinase C oscillations: protein kinase C-dependent receptor phosphorylation is not required. *J Biol Chem* **276**: 35900–35908.

Dale LB, Bhattacharya M, Anborgh PH, Murdoch B, Bhatia M, Nakanishi S, and Ferguson SSG (2000) G protein-coupled receptor kinase-mediated desensitization of metabotropic glutamate receptor 1A protects against cell death. *J Biol Chem* **275**:38213–38220.

Dhami GK and Ferguson SSG (2006) Regulation of metabotropic glutamate receptor signaling, desensitization and endocytosis. *Pharmacol Ther* **111**:260–271.

Dhami GK, Babwah AV, Sterne-Marr R, and Ferguson SSG (2005) Phosphorylation-independent regulation of metabotropic glutamate receptor 1 signaling requires g protein-coupled receptor kinase 2 binding to the second intracellular loop. *J Biol Chem* **280**:24420–24427.

Dhami GK, Dale LB, Anborgh PH, O'Connor-Halligan KE, Sterne-Marr R, and Ferguson SSG (2004) G Protein-coupled receptor kinase 2 regulator of G protein signaling homology domain binds to both metabotropic glutamate receptor 1a and Galphaq to attenuate signaling. *J Biol Chem* **279**:16614–16620.

Dingledine R, Borges K, Bowie D, and Traynelis SF (1999) The glutamate receptor ion channels. *Pharmacol Rev* **51**:7–61.

Durinck S, Ho C, Wang NJ, Liao W, Jakkula LR, Collisson EA, Pons J, Chan SW, Lam ET, and Chu C, et al. (2011) Temporal dissection of tumorgenesis in primary cancers. *Cancer Discov* **1**:137–143.

Emery AC, Pshenichkin S, Takoudjou GR, Grajkowska E, Wolfe BB, and Wroblewski JT (2010) The protective signaling of metabotropic glutamate receptor 1 Is mediated by sustained, beta-arrestin-1-dependent ERK phosphorylation. *J Biol Chem* **285**:26041–26048.

Ferguson SSG (2007) Phosphorylation-independent attenuation of GPCR signalling. *Trends Pharmacol Sci* **28**:173–179.

Francesconi A and Duvoisin RM (2000) Opposing effects of protein kinase C and protein kinase A on metabotropic glutamate receptor signaling: selective desensitization of the inositol trisphosphate/Ca2+ pathway by phosphorylation of the receptor-G protein-coupling domain. *Proc Natl Acad Sci USA* **97**:6185–6190.

Huang S, Cao J, Jiang M, Labesse G, Liu J, Pin JP, and Rondard P (2011) Interdomain movements in metabotropic glutamate receptor activation. *Proc Natl Acad Sci USA* **108**:15480–15485.

Kammermeier PJ (2008) Endogenous homer proteins regulate metabotropic glutamate receptor signaling in neurons. *J Neurosci* **28**:8560–8567.

Kammermeier PJ, Xiao B, Tu JC, Worley PF, and Ikeda SR (2000) Homer proteins regulate coupling of group I metabotropic glutamate receptors to N-type calcium and M-type potassium channels. *J Neurosci* **20**:7238–7245.

Kan Z, Jaiswal BS, Stinson J, Janakiraman V, Bhatt D, Stern HM, Yue P, Haverty PM, Bourgon R, and Zheng J et al. (2010) Diverse somatic mutation patterns and pathway alterations in human cancers. *Nature* **466**:869–873.

Krupnick JG and Benovic JL (1998) The role of receptor kinases and arrestins in G protein-coupled receptor regulation. *Annu Rev Pharmacol Toxicol* **38**:289–319.

Mao L, Yang L, Tang Q, Samdani S, Zhang G, and Wang JQ (2005) The scaffold protein Homer1b/c links metabotropic glutamate receptor 5 to extracellular signal-regulated protein kinase cascades in neurons. *J Neurosci* **25**:2741–2752.

Martino JJ, Wall BA, Mastrantoni E, Wilimczyk BJ, La Cava SN, Degenhardt K, White E, and Chen S (2012) Metabotropic glutamate receptor 1 (Grm1) is an oncogene in epithelial cells. *Oncogene* DOI: 10.1038/onc.2012.471 [published ahead of print].

Nicodemo AA, Pampillo M, Ferreira LT, Dale LB, Cregan T, Ribeiro FM, and Ferguson SSG (2010) Pyk2 uncouples metabotropic glutamate receptor G protein signaling but facilitates ERK1/2 activation. *Mol Brain* **3**:4.

Niswender CM and Conn PJ (2010) Metabotropic glutamate receptors: physiology, pharmacology, and disease. *Annu Rev Pharmacol Toxicol* **50**:295–322.

O'Hara PJ, Sheppard PO, Thøgersen H, Venezia D, Haldeman BA, McGrane V, Houamed KM, Thomsen C, Gilbert TL, and Mulvihill ER (1993) The ligand-binding domain in metabotropic glutamate receptors is related to bacterial periplasmic binding proteins. *Neuron* **11**:41–52.

Ohtani Y, Harada T, Funasaka Y, Nakao K, Takahara C, Abdel-Daim M, Sakai N, Saito N, Nishigori C, and Aiba A (2008) Metabotropic glutamate receptor subtype-1 is essential for in vivo growth of melanoma. *Oncogene* **27**:7162–7170.

Parsons DW, Jones S, Zhang X, Lin JC, Leary RJ, Angenendt P, Mankoo P, Carter H, Siu IM, and Gallia GL et al. (2008) An integrated genomic analysis of human glioblastoma multiforme. *Science* **321**:1807–1812.

Pin JP, Galvez T, and Prézeau L (2003) Evolution, structure, and activation mechanism of family 3/C G-protein-coupled receptors. *Pharmacol Ther* **98**:325–354.

Pollock PM, Cohen-Solal K, Sood R, Namkoong J, Martino JJ, Koganti A, Zhu H, Robbins C, Makalowska I, and Shin SS, et al. (2003) Melanoma mouse model implicates metabotropic glutamate signaling in melanocytic neoplasia. *Nat Genet* **34**:108–112.

Prickett TD, Wei X, Cardenas-Navia I, Teer JK, Lin JC, Walia V, Gartner J, Jiang J, Cherukuri PF, and Molinolo A, et al. (2011) Exon capture analysis of G protein-coupled receptors identifies activating mutations in GRM3 in melanoma. *Nat Genet* **43**:1119–1126.

Quesada V, Conde L, Villamor N, Ordóñez GR, Jares P, Bassaganyas L, Ramsay AJ, Beà S, Pinyol M, and Martínez-Trillos A, et al. (2011) Exome sequencing identifies recurrent mutations of the splicing factor SF3B1 gene in chronic lymphocytic leukemia. *Nat Genet* **44**:47–52.

Ribeiro FM, Ferreira LT, Paquet M, Cregan T, Ding Q, Gros R, and Ferguson SSG (2009) Phosphorylation-independent regulation of metabotropic glutamate receptor 5 desensitization and internalization by G protein-coupled receptor kinase 2 in neurons. *J Biol Chem* **284**:23444–23453.

Roche KW, Tu JC, Petralia RS, Xiao B, Wenthold RJ, and Worley PF (1999) Homer 1b regulates the trafficking of group I metabotropic glutamate receptors. *J Biol Chem* **274**:25953–25957.

Romano C, Yang WL, and O'Malley KL (1996) Metabotropic glutamate receptor 5 is a disulfide-linked dimer. *J Biol Chem* **271**:28612–28616.

Rozengurt E (2007) Mitogenic signaling pathways induced by G protein-coupled receptors. *J Cell Physiol* **213**:589–602.

Shah SP, Roth A, Goya R, Oloumi A, Ha G, Zhao Y, Turashvili G, Ding J, Tse K, and Haffari G, et al. (2012) The clonal and mutational evolution spectrum of primary triple-negative breast cancers. *Nature* **486**:395–399.

Shin SS, Namkoong J, Wall BA, Gleason R, Lee HJ, and Chen S (2008) Oncogenic activities of metabotropic glutamate receptor 1 (Grm1) in melanocyte transformation. *Pigment Cell Melanoma Res* **21**:368–378.

Shiraishi-Yamaguchi Y and Furuichi T (2007) The Homer family proteins. *Genome Biol* **8**:206.

Shiraishi-Yamaguchi Y, Sato Y, Sakai R, Mizutani A, Knöpfel T, Mori N, Mikoshiba K, and Furuichi T (2009) Interaction of Cupidin/Homer2 with two actin cytoskeletal regulators, Cdc42 small GTPase and Drebrin, in dendritic spines. *BMC Neurosci* **10**:25 DOI: 10.1186/1471-2202-10-25.

Sjöblom T, Jones S, Wood LD, Parsons DW, Lin J, Barber TD, Mandelker D, Leary RJ, Ptak J, and Silliman N, et al. (2006) The consensus coding sequences of human breast and colorectal cancers. *Science* **314**:268–274.

Speyer CL, Smith JS, Banda M, DeVries JA, Mekani T, and Gorski DH (2012) Metabotropic glutamate receptor-1: a potential therapeutic target for the treatment of breast cancer. *Breast Cancer Res Treat* **132**:565–573.

Stransky N, Egloff AM, Tward AD, Kostic AD, Cibulskis K, Sivachenko A, Kryukov GV, Lawrence MS, Sougnez C, and McKenna A, et al. (2011) The mutational landscape of head and neck squamous cell carcinoma. *Science* **333**:1157–1160.

Tadokoro S, Tachibana T, Imanaka T, Nishida W, and Sobue K (1999) Involvement of unique leucine-zipper motif of PSD-Zip45 (Homer 1c/vesl-1L) in group 1 metabotropic glutamate receptor clustering. *Proc Natl Acad Sci USA* **96**:13801–13806.

Teh J and Chen S (2012) mGlu receptors and cancerous growth. *Wiley Interdiscip Rev Membr Trasp Signal* **1**:211–220.

Thandi S, Blank JL, and Challiss RA (2002) Group-I metabotropic glutamate receptors, mGlu1a and mGlu5a, couple to extracellular signal-regulated kinase (ERK) activation via distinct, but overlapping, signalling pathways. *J Neurochem* **83**:1139–1153.

Tu JC, Xiao B, Yuan JP, Lanahan AA, Leoffert K, Li M, Linden DJ, and Worley PF (1998) Homer binds a novel proline-rich motif and links group 1 metabotropic glutamate receptors with IP3 receptors. *Neuron* **21**:717–726.

Willard MD, Lajiness ME, Wulur IH, Feng B, Swearingen ML, Uhlik MT, Kinzler KW, Velculescu VE, Sjöblom T, and Markowitz SD, et al. (2012) Somatic mutations in CCK2R alter receptor activity that promote oncogenic phenotypes. *Mol Cancer Res* **10**:739–749.

Address correspondence to: Dr. S. S. G. Ferguson, Robarts Research Institute, University of Western Ontario, 100 Perth Dr., London, Ontario, Canada, N6A 5K8. E-mail: ferguson@robarts.ca